

Entropic effects, shape, and size of mixed micelles formed by copolymers with complex architecturesAndreas Kalogirou,¹ Leonidas N. Gergidis,² Othonas Moulτος,^{1,3} and Costas Vlahos^{1,*}¹*Department of Chemistry, University of Ioannina, 45110 Ioannina, Greece*²*Department of Materials Science & Engineering, University of Ioannina, 45110 Ioannina, Greece*³*Chemical Engineering Program, Texas A&M University at Qatar, P.O. Box 23874, Doha, Qatar*

(Received 12 July 2015; published 20 November 2015)

The entropic effects in the comicellization behavior of amphiphilic AB copolymers differing in the chain size of solvophilic A parts were studied by means of molecular dynamics simulations. In particular, mixtures of miktoarm star copolymers differing in the molecular weight of solvophilic arms were investigated. We found that the critical micelle concentration values show a positive deviation from the analytical predictions of the molecular theory of comicellization for chemically identical copolymers. This can be attributed to the effective interactions between copolymers originated from the arm size asymmetry. The effective interactions induce a very small decrease in the aggregation number of preferential micelles triggering the nonrandom mixing between the solvophilic moieties in the corona. Additionally, in order to specify how the chain architecture affects the size distribution and the shape of mixed micelles we studied star-shaped, H-shaped, and homo-linked-rings–linear mixtures. In the first case the individual constituents form micelles with preferential and wide aggregation numbers and in the latter case the individual constituents form wormlike and spherical micelles.

DOI: [10.1103/PhysRevE.92.052601](https://doi.org/10.1103/PhysRevE.92.052601)

PACS number(s): 82.35.Lr, 82.20.Wt, 82.35.Jk, 82.70.Uv

I. INTRODUCTION

Recent literature has been enriched by studies of the micellization properties of amphiphilic copolymers with complex architectures such as miktoarm stars [1], dendritic [2–4], H-shaped [5,6], super-H-shaped [7], star-block [8], theta [9,10], figure-eight-shaped [10–13] and linked rings [10]. Interesting examples, demonstrating the significant effect of copolymer architecture on the micellization properties are the cases of H-shaped [5,6] and super-H-shaped [7] copolymers. When the solvophobic content varies between 10% and 33% of the total molecular weight, the formed micelles do not have a preferential aggregation number but follow a non–bell-shaped distribution with a wide range of aggregation numbers.

Recent studies [4,8] have shown that copolymer architecture can also strongly influence the shape of the micelles, which can be very different from the usual spherical one. A characteristic example is the high arm number star-block copolymers with solvophilic interior blocks [8]. The dense solvophilic core enforces the melted solvophobic blocks to create multiple aggregative domains (sticky patches) on the periphery of the core. When the number of sticky domains equals 2, the star-block copolymer chains are interconnected through these sticky domains leading the formation of wormlike superstructures with wide aggregation numbers [8]. The increase of the number of aggregative domains triggers the formation of highly branched superstructures. Similar micelle shapes are also obtained from theta-shaped [9,10] and linked-rings copolymers [10].

Zhulina *et al.* [14–16], using scaling theories, have described in a systematic way the effect of composition and architecture of copolymer moieties on the equilibrium shape of aggregates in dilute solutions. For pure diblock copolymers, it was theoretically predicted, and confirmed by experiments [14], that the increase of the insoluble

block's molecular weight changes the morphology of the micelles from spherical to wormlike or cylindrical. Zhulina and co-workers [14–16] have shown that the nonspherical micelles are thermodynamically stable when the dimensions of the insoluble core are comparable to or greater than the corona. For miktoarm star copolymers it was shown that the increase of insoluble arms leads to destabilization of the spherical morphology and promotes the transition to cylindrical or lamellar-shape aggregates. The relative shift in binodal curve, due to the increase of solvophobic arms, can be described by a universal power law, independent of the nature of soluble arms. Similar trends were predicted for the case of cyclization of insoluble blocks in the linear diblock copolymer.

In both cases, the alteration of the spherical morphology could be explained by the increased entropic penalty introduced because more linear or ring solvophobic blocks stretch to fit into the micellar core.

A preferable and efficient approach of controlling the size of micelles, avoiding complicated synthetic schemes, is blending two or more amphiphilic copolymers, differing in the length or the type of the solvophilic part. This approach leads to mixed micelles with the desired properties. Another advantage of the comicellization is the improved thermodynamic stability of the micelle even by adding a small amount of copolymers with lower critical micelle concentration (cmc) values [17,18]. In an ideal blend, the critical micelle concentration and the aggregation number of the mixed micelle can be mathematically obtained from the cmc, the aggregation number, and the molar fractions of its constituents [19].

Experimental studies of linear-cyclic diblock copolymer blends have shown another interesting feature of blending which is the ability of controlling the morphology of micelles by adjusting the relative amount of each copolymer [20]. Pure ring copolymer micelles are wormlike cylindrical objects formed by unidirectional self-assembly of sunflowerlike micelles. On the contrary, linear diblock copolymers, having the same composition, form spherical micelles [20]. In a

*cvlahos@cc.uoi.gr

blend, the formation of the cylindrical aggregates is inhibited by the presence of the linear diblock copolymer (even at 5% of the total polymer mass) because the incorporation of the latter molecule stabilizes the elementary micelles against unidirectional self-assembly which leads the formation of cylindrical micelles.

In a previous paper [21] we reported important entropic effects [22–31] associated with comicellization of chemically identical copolymers differing in chain architecture of solvophilic or solvophobic parts. In particular, we studied linear-star, and star-star mixtures. The simulation results revealed that the cmc for linear-star mixtures shows a positive deviation from the ideal behavior. On the contrary, the star-star mixtures follow the ideal behavior taking into account the statistical uncertainty. The interaction parameters obtained from the activity coefficients were attributed to the effective interactions between copolymers originated from the architectural asymmetry. These interactions are higher in the case of linear-star mixtures and lower in star-star mixtures. The effective interactions slightly decrease the preferential aggregation number of the micelles in linear-star mixtures while for the star-star mixtures the preferential aggregation number can be satisfactorily predicted by the mixing rule. The radial distribution functions and snapshot analysis, for all the mixtures, revealed nonrandom mixing of the solvophilic parts of the copolymers in the corona.

To shed light on some unresolved issues regarding the comicellization behavior of copolymer mixtures we employed molecular dynamics simulations using a Langevin thermostat. In particular, we studied star-star mixtures where the individual constituents differ only in the molecular weight of the solvophilic part in order to elucidate the effect of size asymmetry on the comicellization. Additionally, in order to specify how the chain architecture affects the size distribution and the shape of mixed micelles we studied star-shaped, H-shaped, and homo-linked-rings–linear mixtures. In the first case the individual constituents form micelles with preferential and wide aggregation numbers and in the latter case the individual constituents form micelles with wormlike and spherical micelles. The properties of interest in this study are the critical micelle concentration, the mean aggregation number, the shape of the micelle which is expressed by the shape anisotropy κ^2 , the thickness of the corona H , and the solvophobic core radius R_c .

II. MODEL

We employed a coarse-grained model to represent the amphiphilic copolymer chains used in this study. A group of atoms was modeled as a bead with diameter σ . Bead-bead interactions were calculated by means of a truncated Lennard-Jones potential:

$$U_{LJ}(r_{ij}) = \begin{cases} 4\varepsilon \left[\left(\frac{\sigma}{r_{ij}} \right)^{12} - \left(\frac{\sigma}{r_{ij}} \right)^6 \right] - \left(\frac{\sigma}{r_{ij}} \right)^{12} + \left(\frac{\sigma}{r_{ij}} \right)^6, & r_{ij} \leq r_{cij} \\ 0, & r_{ij} > r_{cij} \end{cases}, \quad (1)$$

where ε is the well depth and r_{cij} is the cutoff radius. Different beads were connected with finitely extensible nonlinear elastic (FENE) bonds. A key physical characteristic of polymer molecules is that the chains cannot cross. The FENE potential inherently achieves this, being harmonic at its minimum, while the bonds cannot be stretched beyond a maximum length determined by R_0 . The FENE potential is expressed as

$$U_{\text{Bond}}(r_{ij}) = \begin{cases} -0.5kR_0^2 \ln \left[1 - \left(\frac{r_{ij}}{R_0} \right)^2 \right], & r_{ij} \leq R_0 \\ \infty, & r_{ij} > R_0 \end{cases}, \quad (2)$$

where r_{ij} is the distance between beads i and j , $k = 25 T \varepsilon / \sigma^2$, and R_0 is the maximum extension of the bond ($R_0 = 1.5 \sigma$). These parameters [32] prevent chain crossing by ensuring an average bond length of 0.97σ . The solvent molecules are considered implicitly. The short time steps needed to model the solvent's behavior (the fast motion) restrict the time scales that may be sampled, thereby limiting the information that can be obtained for the slower motion of the copolymer. Molecular dynamics simulation with Langevin thermostat allows the statistical treatment of the solvent, incorporating its influence on the copolymer by a combination of random forces and frictional terms. The friction coefficient and the random force couple the simulated system to a heat bath and therefore the simulation has canonical ensemble (NVT) constraints. The equation of motion of each bead i of mass m in the simulation

box follows the Langevin equation:

$$m_i \ddot{\mathbf{r}}_i(t) = -\nabla \sum_j [U_{LJ}(r_{ij}) + U_{\text{Bond}}(r_{ij})] - m_i \xi \dot{\mathbf{r}}_i(t) + \mathbf{F}_i(t), \quad (3)$$

where m_i , r_i , and ξ are the mass, the position vector, and the friction coefficient of the i bead, respectively. The friction coefficient is equal to $\xi = 0.5 \tau^{-1}$, with $\tau = \sigma \sqrt{m/\varepsilon}$. The random force vector F_i is assumed to be Gaussian, with zero mean, and satisfies the equation

$$\langle \mathbf{F}_i(t) \mathbf{F}_j(t') \rangle = 6k_B T m \xi \delta_{ij} \delta(t - t'), \quad (4)$$

where k_B is the Boltzmann constant and T is the temperature.

In amphiphilic copolymers A beads are considered solvophilic and B beads solvophobic. In all simulations presented here the solvophobic part B contained 30 beads, while the length of the A block varied. The individual constituents of the mixtures are (a) linear diblock copolymers with 16 solvophilic beads denoted as $A_{16}B_{30}$; (b) miktoarm star copolymers with 120, 64, and 32 solvophilic beads which are distributed in two $(A_{60})_2$ or four branches $(A_{16})_4$, $(A_8)_4$; (c) H-shaped copolymers of the type $(A_{30})_2B_{30}(A_{30})_2$ with two branches containing 30 beads connected to one end of the solvophobic bridge B , and the other two of the same length branches, connected to the opposite end of the solvophobic bridge; and (d) homo-linked-rings copolymer

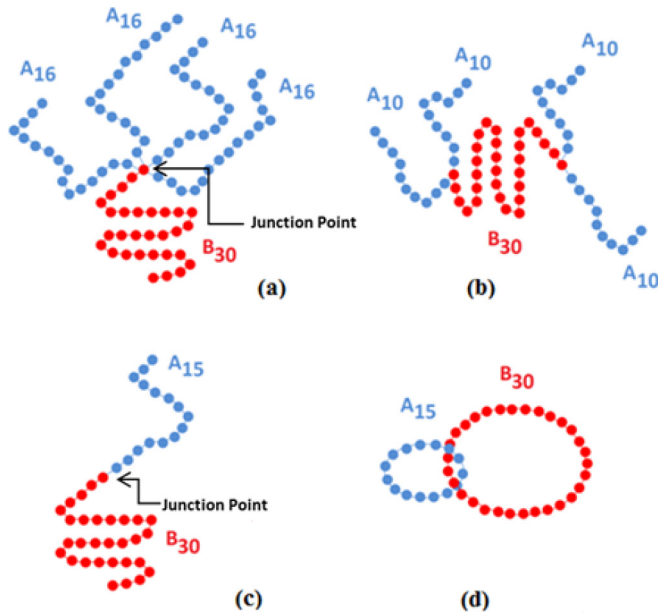


FIG. 1. (Color online) Cartoon representation of (a) miktoarm star copolymer $(A_{16})_4B_{30}$, (b) H-shaped copolymer $((A_{30})_2B_{30}(A_{30})_2)$, (c) linear diblock copolymers $A_{15}B_{30}$, and (d) homo-linked-rings copolymer $A_{15}B_{30}$.

$A_{16}B_{30}$ which contains a solvophilic ring with 16 beads and a solvophobic with 30 beads. Cartoon representations of some of the aforementioned copolymer architectures are illustrated in Fig. 1.

Three binary mixtures of copolymers were studied in the present work. Namely, the mixture of (i) star $(A_{16})_4B_{30}$ with star $(A_8)_4B_{30}$, (ii) star $(A_{60})_2B_{30}$ with H-shaped $(A_{30})_2B_{30}(A_{30})_2$, and (iii) homo-linked-ring $A_{16}B_{30}$ with linear $A_{16}B_{30}$. We have chosen the aforementioned molecular weights in order to obtain the desired shape or mass distribution (wormlike micelles from homo-linked-ring copolymers and non-bell-shaped mass distribution from H-shaped copolymers), while for the remaining cases the chosen ratio of solvophobic to solvophilic units γ allows the systems to equilibrate faster.

The molar fractions of the two individual constituents in the mixture, $[X_1]$ and $[X_2]$, are given by

$$[X_1] = \frac{N_1}{N_1 + N_2}, \quad (5)$$

$$[X_2] = 1 - [X_1], \quad (6)$$

where N_1 and N_2 are the number of chains of the two different copolymers in the mixture. In every case studied we had $[X_1] = 1, 0.75, 0.5, 0.25,$ and 0 while $[X_2]$ values were, set respectively, according to Eq. (6). The total copolymer concentration, $[X]$, is given by

$$[X] = \frac{N_1M_1 + N_2M_2}{V}, \quad (7)$$

where M_1 and M_2 are the molecular weights of copolymers of type 1 and 2, respectively, and V is the total volume of the simulation box.

Molecular dynamics simulations with a Langevin thermostat were performed in a cubic box with periodic boundary conditions, using the open-source massive parallel simulator LAMMPS [33]. The reduced temperature of the simulation T^* was set to $T^* = k_B T / \varepsilon = 1.8$. This choice of temperature allows the studied systems to have both micelles and free molecules [3]. If the temperature is very low, the studied system contains only aggregates and no free molecules, while if the temperature is very high, the studied system contains only free molecules and no aggregates. Different cutoff distances in the Lennard-Jones potential were used [3,4] to describe the interactions between copolymer units. The B - B interaction had an attractive potential with cutoff radius $r_{cij} = 2.5\sigma$ while the A - A and A - B interactions were considered repulsive and had cutoff radii $r_{cij} = 2^{1/6}\sigma$. In the latter case the Lennard-Jones potential is shifted by ε . For the sake of simplicity, all types of beads were considered to have the same mass ($m = 1$) and diameter ($\sigma = 1$). Copolymers were assumed to reside to the same micelle if the distance between any two nonbonded solvophobic beads B , belonging to different chains, was found within 1.5σ . The aforementioned criterion has been adopted by the literature for the description of the micellization process where this distance corresponds to the maximum extension of the FENE bonds [3,4]. In all simulations we set $\varepsilon = 1$.

In the current study, systems containing $N_1 + N_2 = 125$ copolymer chains were simulated for the calculation of the cmc values. All other properties were obtained from systems with $N_1 + N_2 = 1000$ chains at total copolymer concentration $[X] = 0.12$ where most aggregates are formed [3]. The system size was chosen so as to prevent the largest micelles from having a radius of gyration greater than one-fourth of the box side length. The use of one quarter of the simulation box side proved to be a sufficient condition to avoid interaction of chains and micelles with their images and therefore no system size effects were observed for all the calculated quantities reported in this paper.

In order to avoid bond crossing at the desired concentration, copolymer chains of types 1 and 2 were initially arranged on a lattice box. The energy of the chains was minimized and then the lattice box was replicated in order to obtain the desired number of chains. We performed one million time steps with integration step $\Delta t = 0.008\tau$ setting all cutoff radii equal to $r_{cij} = 2^{1/6}\sigma$ in order to eliminate any bias introduced from the initial conformation. Then, the system was allowed to equilibrate for ten million steps. The simulation was subsequently conducted for ten million steps for the systems with 125 copolymer chains, and 100 million steps for the larger systems with 1000 amphiphiles. The duration of the simulation was evaluated by calculating the tracer autocorrelation function:

$$C(t) = \frac{\langle N(t_0 + t)N(t_0) \rangle - \langle N(t_0) \rangle^2}{\langle N^2(t_0) \rangle - \langle N(t_0) \rangle^2}, \quad (8)$$

where $N(t)$ is the number of molecules in the micelle in which the copolymer resides at time t . All copolymers were considered as tracers, and every time step as a time origin t_0 . The characteristic relaxation time t_{relax} is defined as the required time for $C(t)$ to reach the value reported in Ref. [3] of e^{-1} . In Fig. 2 we report the tracer autocorrelation function for various systems studied. Each simulation was conducted for at

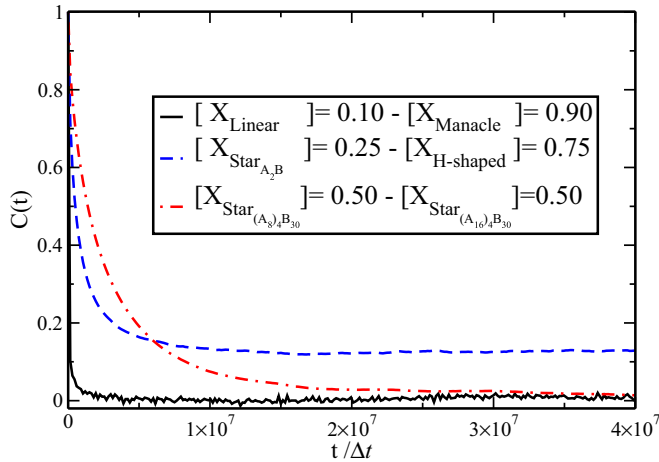


FIG. 2. (Color online) Tracer autocorrelation function $C(t)$ for different copolymer mixtures.

least $10t_{\text{relax}}$ in order to have ten independent conformations. The properties of interest were calculated as averages from 1000 and 2000 snapshots for the systems with 125 and 1000 chains, respectively.

III. RESULTS AND DISCUSSION

A. Critical micelle concentration

The critical micelle concentration (cmc) is traditionally depicted [3] by plotting the free (nonassociated) copolymer monomers concentration $[F]$ as a function of the total copolymer monomers concentration $[X]$. In the case of amphiphilic copolymer mixtures, where mixed aggregates are formed, the maximum of the total free chain concentration including both types of copolymers determines the cmc. Figure 3 shows plots of the total free copolymer concentration against the total copolymer concentration $[X]$ for the simulated binary mixtures of star $(A_{16})_4B_{30}$ –star $(A_8)_4B_{30}$, star $(A_{60})_2B_{30}$ –H-shaped $(A_{30})_2B_{30}(A_{30})_2$, and linear $A_{16}B_{30}$ –homo-linked-rings $A_{16}B_{30}$ for various molar fractions of the two types of amphiphilic copolymers. The cmc values calculated from Fig. 3 are given in Table I.

The cmc value of pure miktoarm copolymer $(A_8)_4B_{30}$ is 0.0089 which is lower than the value 0.0178 of pure star $(A_{16})_4B_{30}$. However, in the micelles formed only by $(A_8)_4B_{30}$ copolymers the steric interactions between the short four arms in the solvophilic corona are weaker compared to the respective interactions between the much longer solvophilic arms of miktoarm copolymer $(A_{16})_4B_{30}$.

According to the molecular theory of micellization [17] the driving force of aggregation is the change in the Gibbs free energy g_{mic} associated with the transfer of n unimers (free chains) from the solution to a micelle. The stronger steric interactions in the corona lead to higher g_{mic} and, according to the theory, to higher cmc values. Analysis of star $(A_{16})_4B_{30}$ –star $(A_8)_4B_{30}$ mixtures revealed the formation of mixed micelles. Initially, small aggregates of $(A_8)_4B_{30}$ miktoarm star chains are formed and, later on, are enriched with $(A_{16})_4B_{30}$ chains. The steric penalty needed to overcome transferring a free $(A_{16})_4B_{30}$ miktoarm star chain from the solution to a

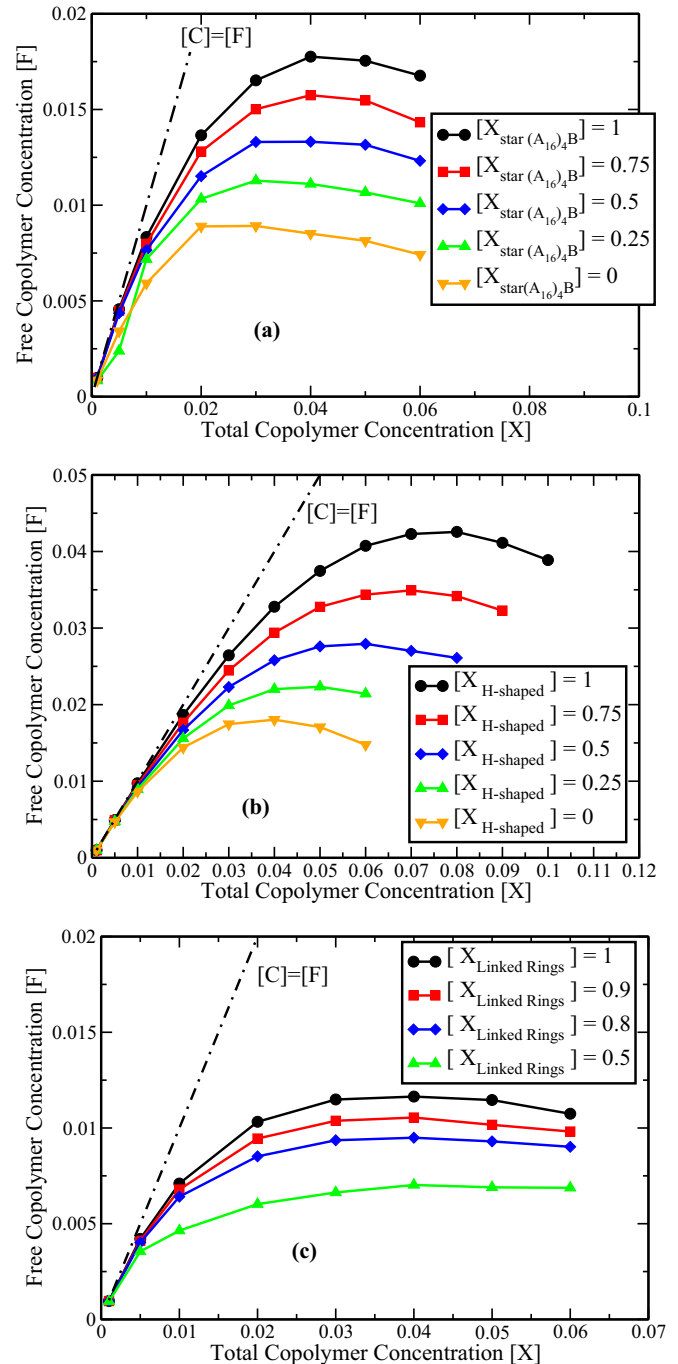


FIG. 3. (Color online) Plots of the total free copolymer concentration against the total copolymer concentration $[X]$ for the simulated binary mixtures of (a) star $(A_{16})_4B_{30}$ –star $(A_8)_4B_{30}$, (b) star $(A_{60})_2B_{30}$ –H-shaped $(A_{30})_2B_{30}(A_{30})_2$, and (c) linear $A_{16}B_{30}$ –homo-linked-rings $A_{16}B_{30}$ at different molar fractions of two types of amphiphilic copolymers.

mixed micelle is smaller compared to the respective steric penalty for the insertion of a free $(A_{16})_4B_{30}$ miktoarm star chain in a small aggregate, formed by pure $(A_{16})_4B_{30}$ miktoarm star copolymer chains. Thus, the formation of mixed micelles is thermodynamically favored with g_{mic} values lying between the values of pure $(A_8)_4B_{30}$ and pure $(A_{16})_4B_{30}$ miktoarm star micelles. This leads to the increase of cmc values of the

TABLE I. Critical micelle concentration (cmc) values for different copolymer mixtures.

Mixture	M_w	γ	cmc
Star $(A_{16})_4 B_{30}$ –star $(A_8)_4 B_{30}$	94/62	0.47/0.94	
$[X_{(A_{16})_4 B_{30}}] = 1$			0.0178
$[X_{(A_{16})_4 B_{30}}] = 0.75$			0.0157
$[X_{(A_{16})_4 B_{30}}] = 0.5$			0.0133
$[X_{(A_{16})_4 B_{30}}] = 0.25$			0.0113
$[X_{(A_{16})_4 B_{30}}] = 0$			0.0089
Star $(A_{60})_2 B_{30}$ –H $(A_{30})_2 B_{30}(A_{30})_2$	150	0.25	
$[X_{(A_{30})_2 B_{30}(A_{30})_2}] = 1$			0.0426
$[X_{(A_{30})_2 B_{30}(A_{30})_2}] = 0.75$			0.0350
$[X_{(A_{30})_2 B_{30}(A_{30})_2}] = 0.5$			0.0279
$[X_{(A_{30})_2 B_{30}(A_{30})_2}] = 0.25$			0.0223
$[X_{(A_{30})_2 B_{30}(A_{30})_2}] = 0$			0.0180
Linear $A_{16} B_{30}$ –linked-rings $A_{16} B_{30}$	46	1.875	
$[X_{A_{16} B_{30}}] = 1$			0.0116
$[X_{A_{16} B_{30}}] = 0.9$			0.0105
$[X_{A_{16} B_{30}}] = 0.8$			0.0095
$[X_{A_{16} B_{30}}] = 0.5$			0.0070
$[X_{A_{16} B_{30}}] = 0$			0.0023

mixture with respect to the pure $(A_8)_4 B_{30}$ copolymer solution. As expected the cmc of the mixture increases as the molar fraction of star chains increases (Table I).

A quantitative prediction of mixture cmc C_M can be obtained by the molecular theory of comicellization as [34,35]

$$\frac{1}{C_M} = \frac{[X_1]}{f_1 C_1} + \frac{1 - [X_1]}{f_2 C_2}, \quad (9)$$

where C_1 and C_2 are the cmc of the type 1 and type 2 copolymers and f_1, f_2 are the activity coefficients of the amphiphilics taking into account the nonideality of the interactions between molecules of different types [36]. All mixtures reported in the present study are composed of chemically identical copolymers (same type of interactions), differing only in the molecular weight of the solvophilic part and therefore the activity coefficients for both components are equal to unity.

The cmc values of the star $(A_{16})_4 B_{30}$ –star $(A_8)_4 B_{30}$ for star copolymer molar fraction $[X_{\text{star}(A_{16})_4 B_{30}}] = 0, 0.25, 0.5, 0.75,$ and 1 are illustrated in Fig. 4(a). In the same figure the analytical results obtained from Eq. (9) with unity activity coefficients are also presented. It can be observed that there is a small deviation from the ideal behavior which becomes even more pronounced as the molar fraction of $(A_{16})_4 B_{30}$ miktoarm star copolymer increases. The simulation results revealed the presence of effective interactions, between the $(A_{16})_4 B_{30}$ and $(A_8)_4 B_{30}$ chemically identical copolymers. Both miktoarm star copolymers contain the same solvophobic part (a linear branch with 30 beads), and thus the nonidealities should originate from the solvophilic corona. The effective interactions take place between the four short arms of $(A_8)_4 B_{30}$ and the chemically identical four long arms of $(A_{16})_4 B_{30}$. The effective interactions parameter u can be obtained from the definition of the activity coefficients [36] $f_1 = \exp\{u(1 - [X_1])^2\}$ and $f_2 = \exp(u[X_1]^2)$. According to Eq. (9) and the expressions for the

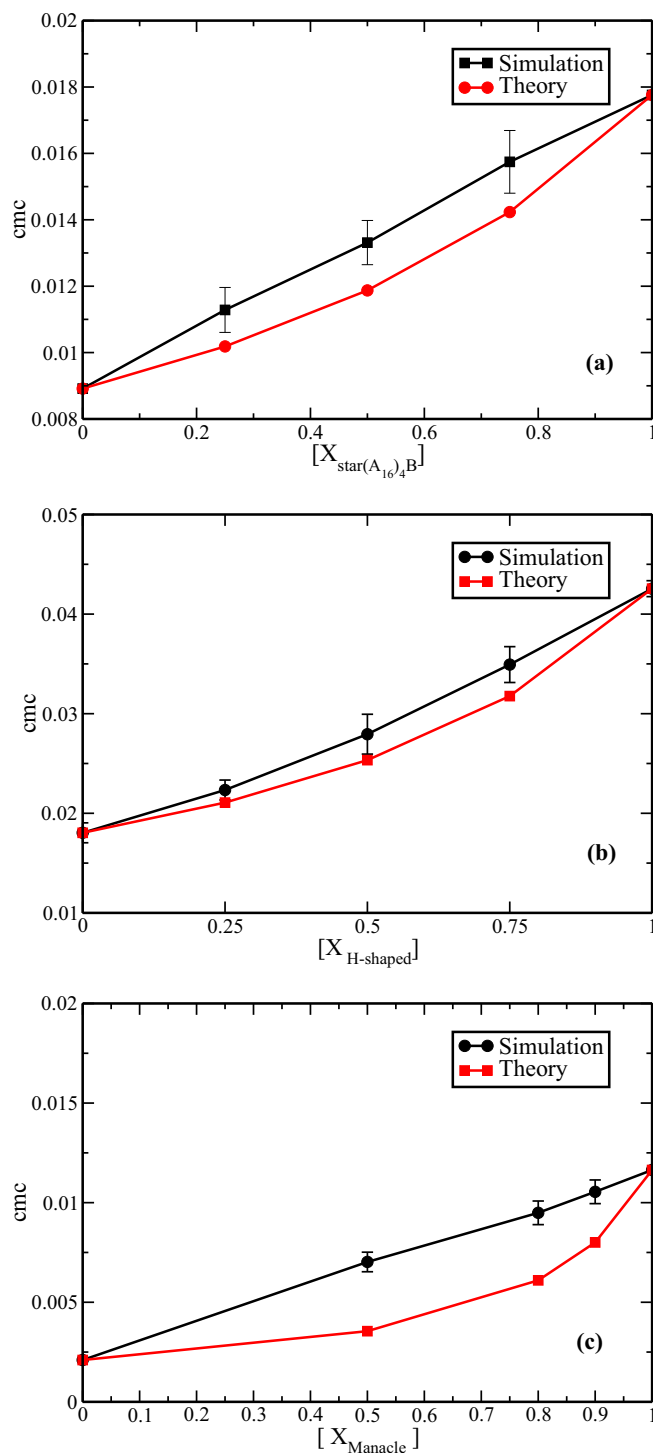


FIG. 4. (Color online) Plots of the cmc values of (a) star $(A_{16})_4 B_{30}$ –star $(A_8)_4 B_{30}$ mixtures with respect to molar fraction of star copolymer $(A_{16})_4 B_{30}$, (b) star $(A_{60})_2 B_{30}$ –H-shaped $(A_{30})_2 B_{30}(A_{30})_2$ mixture, (c) linear $A_{16} B_{30}$ –homo-linked-rings $A_{16} B_{30}$. Within the same figure the analytical results obtained from Eq. (9) with unity activity coefficients are also shown.

activity coefficients f_1 and f_2 one can obtain the parameter u , by fitting the simulation values to $1/C_M$. Thus we obtain $u \approx 0.5$. The aforementioned u value lies between the reported values for the effective interaction for the linear $A_{63} B_{30}$ –

star $(A_{21})_3B_{30}$ ($u \approx 0.6$) and star $(A_{32})_2B_{30}$ –star $(A_{16})_4B_{30}$ ($u \approx 0.1$) mixtures in our previous simulation work [21]. Scaling theories developed by Zhulina and Borisov [14–16] predict the cmc values of pure micelles as a function of the hydrophilic and hydrophobic block lengths, N_A and N_B .

More specifically, for crew-cut micelles, where the micellar core radius is larger than the thickness of the corona, the logarithm of cmc is related to the solvophilic arm length and can be obtained by $\ln(\text{cmc}) \sim N_A^{-2/3}$. The power law obtained from the $(A_{16})_4B_{30}$ and $(A_8)_4B_{30}$ star copolymers simulation reads as $\ln(\text{cmc}) \sim N_A^{-0.2}$. The discrepancy between scaling and simulation results could be attributed to the low molecular weights used for the simulations of miktoarm copolymers.

The simulation results for star $(A_{60})_2B_{30}$ –H-shaped $(A_{30})_2B_{30}(A_{30})_2$ mixtures are illustrated in Fig. 4(b). In this system we observe the highest difference between the cmc values of pure components. The free energy change g_{pack} , associated with constraining both ends of the solvophobic part B to lie in the periphery in H-shaped copolymers, is higher than the respective energy change associated with constraining the one end of the solvophobic part of the miktoarm copolymer. In addition, the H-shaped copolymer contains twice the branches of the star $(A_{60})_2B_{30}$ resulting in a higher g_{st} energetic penalty. In this mixture the increase of H-shaped copolymer molar fraction leads to higher cmc values than the ones obtained from the ideal model [Eq. (9)]. This finding can be attributed to the significant asymmetry between these two architectures. The interaction parameter u obtained from the activity coefficients is $u \approx 0.4$. However, in this mixture the molecular weight of the copolymers ($M_w = 150$) is higher than the respective molecular weight of the previous mixtures ($M_w = 93$), which indicates that for shorter chains the deviation from ideality should be higher.

The results of the linear $A_{16}B_{30}$ –homo-linked-rings $A_{16}B_{30}$ mixture are presented in Fig. 4(c). It can be observed that the simulation values significantly deviate from the respective theoretical values. The interaction parameter u obtained from the activity coefficients, reflecting the effective repulsions between the solvophilic ring and linear moieties in the corona, is $u \approx 2.4$, a value much higher than the respective value for linear-star mixtures ($u \approx 0.7$). This result is in agreement with the analytical theory of Vlahos and Kosmas [29] for linear-ring blends. The effective Flory parameter χ_{eff} for linear-ring and linear-star chemically identical blends for volume fraction 0.5 and $M_w = 300$ was found to be 1×10^{-4} and 8×10^{-6} , respectively.

B. Micelle size and shape

For the characterization of the mixed micelles, formed by the aforementioned binary mixtures, we calculated the following quantities: the aggregation number N , and the radii of gyration of the core $\langle R_g^2 \rangle_{\text{core}}$ and of the whole aggregate $\langle R_g^2 \rangle_{\text{micelle}}$, as well as the resulting thickness H and the shape anisotropies $\kappa_{\text{micelle}}^2$, κ_{core}^2 . All these properties were calculated on the most concentrated solutions with $[X] = 0.12$, where most aggregates are formed. Our results on the mass distributions of micelles, for different molar fractions of constituent copolymers in the mixtures, are illustrated in Fig. 5,

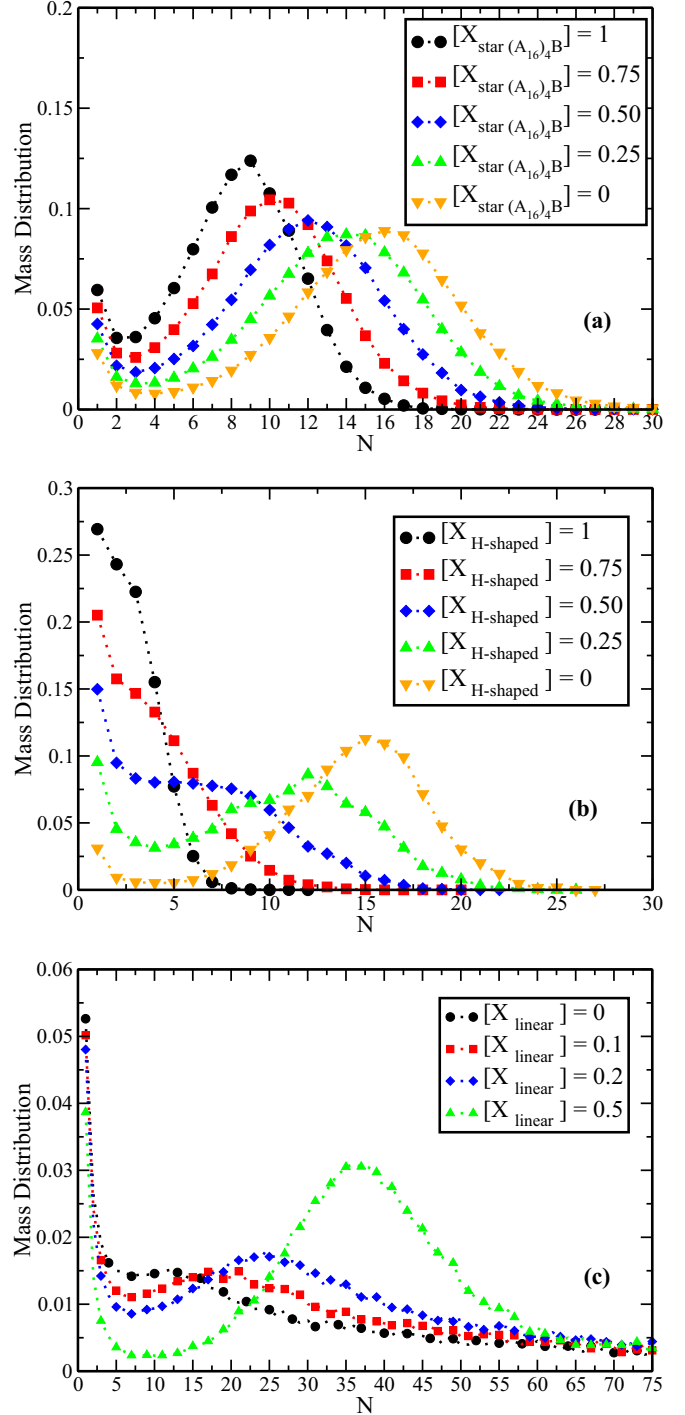


FIG. 5. (Color online) Mass distributions of micelles in the mixtures (a) star $(A_{16})_4B_{30}$ –star $(A_8)_4B_{30}$, (b) star $(A_{60})_2B_{30}$ –H-shaped $(A_{30})_2B_{30}(A_{30})_2$ mixture, (c) linear $A_{16}B_{30}$ –homo-linked-rings $A_{16}B_{30}$ as a function of the aggregation number N_p .

while the shape characteristics of the most probable micelles are summarized in Table II.

For the case of star $(A_{16})_4B_{30}$ –star $(A_8)_4B_{30}$ mixtures, the mass distribution depends on the molar fraction as it can be observed in Fig. 5(a). The pure miktoarm star $(A_{16})_4B_{30}$ has smaller preferential aggregation number N_p than the $(A_8)_4B_{30}$ counterpart. This reflects the difference in steric

TABLE II. Shape characteristics of the most probable formed aggregates of various mixtures. Standard deviation is inside the parentheses.

System	N_p	$\langle R_g^2 \rangle_{\text{micelle}}$	$\langle R_g^2 \rangle_{\text{core}}$	$\langle \kappa^2 \rangle_{\text{micelle}}$	$\langle \kappa^2 \rangle_{\text{core}}$	H	R_{core}
$(A_{16})_4B_{30}-(A_8)_4B_{30}$							
$[X_{(A_{16})_4B_{30}}] = 1$	9	68.4 (0.3)	21.5 (0.2)	0.050 (0.001)	0.112 (0.002)	4.69 (0.04)	5.98 (0.03)
$[X_{(A_{16})_4B_{30}}] = 0.75$	10	67.1 (0.2)	22.55 (0.08)	0.0489 (0.0005)	0.113 (0.001)	4.45 (0.03)	6.131 (0.004)
$[X_{(A_{16})_4B_{30}}] = 0.50$	12	68.0 (0.2)	24.72 (0.09)	0.05 (0.05)	0.105 (0.001)	4.23 (0.03)	6.419 (0.004)
$[X_{(A_{16})_4B_{30}}] = 0.25$	14	68.5 (0.1)	26.9 (0.2)	0.0443 (0.0008)	0.100 (0.002)	3.980 (0.001)	6.696 (0.007)
$[X_{(A_{16})_4B_{30}}] = 0$	17	106.1 (0.4)	26.3 (0.3)	0.025 (0.001)	0.082 (0.004)	6.67 (0.05)	6.62 (0.04)
$(A_{60})_2B_{30}-(A_{30})_2B_{30}(A_{30})_2$							
$[X_{(A_{30})_2B_{30}(A_{30})_2}] = 0.25$	12	87.9 (0.2)	22.3 (0.1)	0.0351 (0.0009)	0.096 (0.002)	5.99 (0.01)	6.11 (0.02)
$[X_{(A_{30})_2B_{30}(A_{30})_2}] = 0$	15	168.4(0.4)	24.0 (0.1)	0.0236 (0.0008)	0.081 (0.002)	10.42 (0.02)	6.32 (0.01)
Homo-linked-rings $A_{16}B_{30}$ -linear $A_{16}B_{30}$							
$[X_{\text{linear } A_{16}B_{30}}] = 0$	12	46.4 (0.4)	40.3(0.4)	0.18 (0.01)	0.227 (0.007)		
$[X_{\text{linear } A_{16}B_{30}}] = 0.1$	18	59(1)	50(2)	0.167 (0.008)	0.219 (0.009)		
$[X_{\text{linear } A_{16}B_{30}}] = 0.2$	24	67(1)	55(1)	0.15 (0.01)	0.20 (0.01)		
$[X_{\text{linear } A_{16}B_{30}}] = 0.5$	36	71(1)	50(1)	0.069 (0.007)	0.12 (0.01)		

interactions between the solvophilic units in the corona. The larger the solvophilic arms are, the higher is the steric penalty for transferring the large $(A_{16})_4B_{30}$ chains into the micelle. Snapshot analysis of the preferential aggregates reveals that the compositions of the different species are identical to the compositions of the copolymers in the dilute solution. Higher concentration of the large star $(A_{16})_4B_{30}$ chains leads in increased steric interactions in the mixed corona and consequently lowers the micelle's preferential aggregation number.

Therefore, one can interpolate between the two N_p limits. In Fig. 6 the preferential aggregation numbers of micelles are plotted for mixtures with linear copolymer molar fraction $[X_{(A_{16})_4B_{30}}] = 0., 0.25, 0.5, 0.75, 1$. The linear interpolation (mixing rule) describing the ideal mixtures is also presented. From this figure one can observe that the preferential aggregation number of the mixed micelle, N_p , is lower than that of the ideal mixture, due to the effective interactions. These interactions originate from the size asymmetry between the different miktoarm star copolymer chains and become

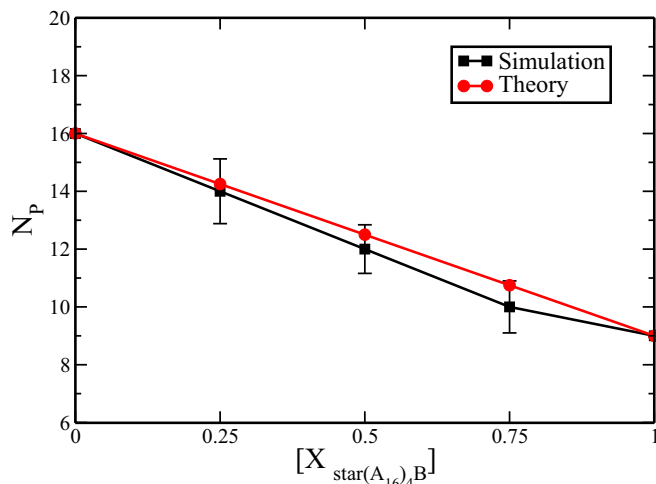


FIG. 6. (Color online) The most probable aggregation numbers of micelles N_p for star $(A_{16})_4B_{30}$ -star $(A_8)_4B_{30}$ mixtures.

stronger as the molar fraction of star $(A_{16})_4B_{30}$ increases. In order to quantitatively describe the mixing between different star solvophilic moieties with long and short branches in the corona, we have calculated the three radial distribution functions $g(r)$, namely, between the junction units of different star $(A_{16})_4B_{30}$ -star $(A_{16})_4B_{30}$, star $(A_{16})_4B_{30}$ -star $(A_8)_4B_{30}$, and star $(A_8)_4B_{30}$ -star $(A_8)_4B_{30}$ chains. The junction unit (Fig. 1) is the point where the solvophilic and solvophobic arms of the miktoarm copolymer connect to each other. After the formation of the micelle the junction points can be located at the periphery of the core, from where the solvophilic moieties of the corona start.

The product $g(r)d^3r$ gives the probability of junction units of the same or different type of miktoarm star copolymer to be found in the volume element d^3r at distance r from a reference junction unit. Moreover, the population of the same or different junction units can be obtained by the following integration: $\int_0^r \rho g(r')4\pi r'^2 dr'$, where ρ is the mean micelle density. In the case of random mixing of miktoarm star copolymers, the three different $g(r)$ functions should coincide. Otherwise nonrandom mixing is obtained, due to the effective repulsive interactions.

As can be observed from Fig. 7, the peaks of the three different $g(r)$ functions for the most probable micelle with $N_p = 14, 12$, and 10 for mixtures with $[X_{(A_{16})_4B_{30}}] = 0.25, 0.5$, and 0.75, respectively, lie in different positions. The $g(r)$ peak corresponding to star $(A_8)_4B_{30}$ -star $(A_8)_4B_{30}$ is lower than that of star $(A_8)_4B_{30}$ -star $(A_{16})_4B_{30}$, indicating lower population of first neighbors of star $(A_8)_4B_{30}$ compared to star $(A_{16})_4B_{30}$. Thus, a nonrandom mixing of the copolymer chains in the corona is obtained. It should be noted, that in all cases, $g(r)$ decays to zero in larger distances, because the micelle has limited extent. This extent is between 15σ and 20σ . The occurrence of peaks at larger distances, beyond the first coordination shell, is more pronounced for star $(A_{16})_4B_{30}$ -star $(A_{16})_4B_{30}$ when $[X_{\text{star}(A_8)_4B_{30}}] = 0.75$. Snapshots have also shown a nonrandom mixing of both copolymers, in a variety of molar fractions [Fig. 8(a)].

Binary mixtures of star $(A_{60})_2B_{30}$ -H-shaped $(A_{30})_2B_{30}(A_{30})_2$ are of great importance. For the chosen molecular weight of the solvophilic part, the micelles'

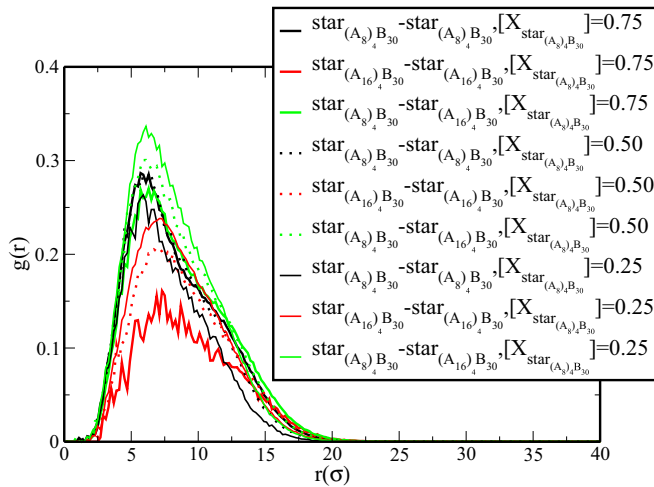


FIG. 7. (Color online) Radial distribution functions of micelles with the most probable aggregation number for star $(A_{16})_4B_{30}$ -star $(A_8)_4B_{30}$ copolymer mixtures.

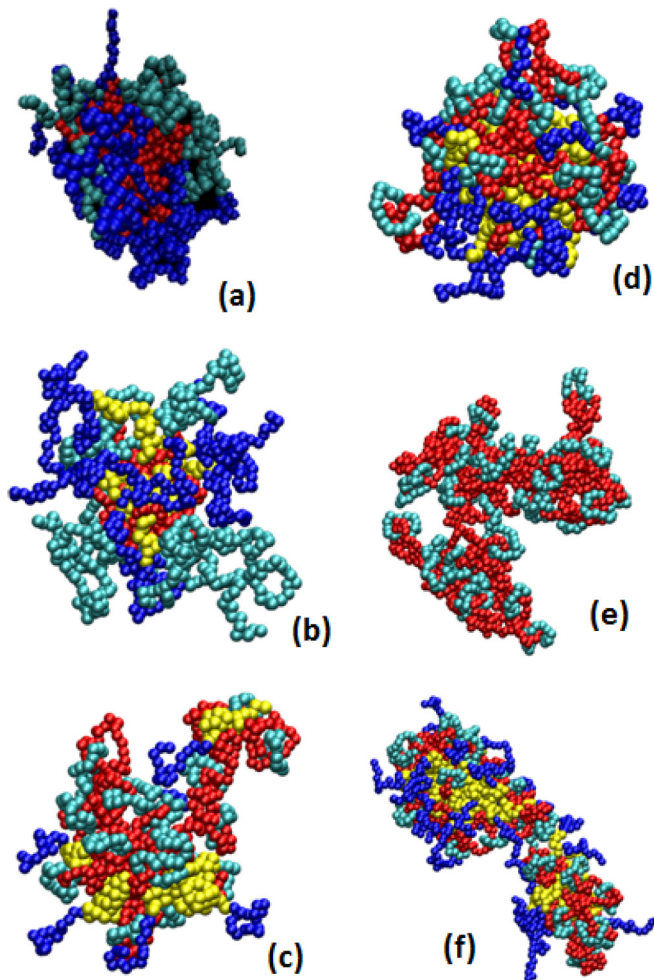


FIG. 8. (Color online) Snapshots of micelles: (a) $[X_{(A_{16})_4B_{30}}] = 0.5$ with $N_p = 12$, (b) $[X_{(A_{60})_2B_{30}}] = 0.5$ with $N_p = 13$, (c) $[X_{\text{linked-rings}}] = 0.8$ with $N_p = 24$, (d) $[X_{\text{linked-rings}}] = 0.5$ with $N_p = 36$, (e) $[X_{\text{linked-rings}}] = 1$ with $N = 36$, (f) $[X_{\text{linked-rings}}] = 0.5$ with $N = 50$.

mass distribution of pure H-shaped copolymer follows a non-bell-shaped distribution as reported by previous experiments [7] and simulations [4], and thus the formed micelles have a wide range of aggregation numbers. On the other hand, the miktoarm star constituent always forms micelles with preferential aggregation number [Fig. 5(b)]. Thus, a reasonable question is *When do the mixed micelles follow a bell-shaped and when a non-bell-shaped distribution?* The simulation results presented in Fig. 5(b) indicate that in mixtures with H-shaped molar fraction $[X_{\text{H-shaped}}] = 0.75$ the mass distribution remains monotonic and mixed micelles with wide aggregation numbers are formed. For mixtures having $[X_{\text{H-shaped}}] = 0.5$ the mass distribution gets almost to a plateau for N ranging from 3 to 9, with a slight maximum at 5, and then slowly decays. Further decrease of H-shaped molar fraction, $[X_{\text{H-shaped}}] = 0.25$, leads in the formation of micelles with preferential aggregation number ($N_p = 12$). The behavior of this mixture can be explained by the progressive reduction of free energy change associated with constraining both ends of the solvophobic part of the H-shaped copolymer to lie in the periphery of the mixed micelle as the molar fraction of miktoarm star copolymer in mixture increases. The aforementioned results are valid for micelles at equilibrium. For solvents with higher selectivity (lower temperature), frozen micelles are obtained and the mass distribution of H-shaped molecules and that of corresponding mixtures may have a very narrow shape.

As already mentioned in the Introduction, experimental results on comicellization of ring diblock copolymers with linear copolymers have shown that mixing can significantly influence the shape of the micelles [21]. Ring copolymers with long solvophobic block form wormlike micelles. In mixtures, even the addition of 5% of linear diblock copolymer was found to be sufficient to stabilize the spherical micelles preventing the formation of wormlike micelles.

The shape of the micelles is an important aspect for some medical applications. Recent studies show that it modulates the degree of particle attachment to macrophages [37]. In particular, prolate spheroids showed the most efficient particle attachment, when compared with spherical particles. Particle shape has also been implicated in increasing circulation time for particles injected into the bloodstream, by aligning with blood flow in a superior fashion to spherical particles and reducing phagocytosis. In our simulations we used a similar structure, the homo-linked-rings copolymers $A_{16}B_{30}$, which contain two chained homopolymer rings with solvophobic to solvophilic ratio $\gamma = 1.9$. The pure homo-linked-rings solution forms wormlike micelles with aggregation number higher than 15 while micelles with smaller aggregation numbers are elongated spheres with κ^2 around 0.18. A small peak is observed at $N_p = 12$ that can be considered as the preferential aggregation number of pure homo-linked-rings micelles [Fig. 5(c), Table II]. Mixtures containing 10% linear diblock copolymers $A_{16}B_{30}$, which have the same molecular weight as homo-linked-rings copolymers, form elongated spherical micelles with preferential aggregation number $N_p = 18$ and $\kappa^2 = 0.18$. Micelles with $N > 25$ are wormlike shaped. Further increase of the linear copolymer molar fraction $[X_{\text{linear}}] = 0.2$ leads to mixed micelles with preferential aggregation number $N_p = 24$ and $\kappa^2 = 0.14$

[Fig. 8(c)], while wormlike micelles are formed for $N > 35$. For mixtures having $[X_{\text{linear}}] = 0.5$ the obtained micelles are spherical with $N_p = 36$ and $\kappa^2 = 0.069$ [Fig. 8(d)] while wormlike micelles are formed for $N > 42$ [Fig. 8(f)]. Since the preferential aggregation number of linear diblock copolymers $A_{16}B_{30}$ is $N_p = 62$ and $\kappa^2 = 0.029$ it can be easily concluded that the preferential aggregation number of the mixtures also follows the mixing rule. For shape comparison purposes, aggregates with $N_p = 36$ are presented together with those of pure homo-linked-rings copolymers having the same N [Figs. 8(d) and 8(e)]. As mentioned in the Introduction, the small size of solvophobic ring in the homo-linked-ring copolymers destabilizes the spherical micelle's shape. The mixing with linear diblock copolymer chains leads to a progressive increase in the size of the solvophobic mixed core, resulting in the stabilization of the spherical micelle's shape.

Many important applications of micelles require the fine-tuning of micellar size and shape. This can be achieved by synthesizing copolymers with specific architectures, total molecular weights, and solvophobic to solvophilic units ratios. For example, the size of micelles used as anticancer drug carriers should be restricted between 20 and 200 nm, in order to be sufficiently large to avoid premature elimination in the kidneys but small enough to enter and circulate into blood vessels [37]. In such cases, a more efficient alternative to synthesis is to blend two or more amphiphilic copolymers, differing in the length or the type of solvophilic part. This leads to the formation of mixed micelles with the desired geometrical characteristics, avoiding complicated synthetic schemes. Our study aims towards the effective development of such important alternatives and gives a qualitative description of the different micellar fine-tuning techniques.

IV. CONCLUSIONS

The entropic effects on the micellization behavior of amphiphilic AB copolymers arising from the size asymmetry of solvophilic A parts were studied by means of molecular dynamics simulations with a Langevin thermostat. In particular, we studied star $(A_{16})_4B_{30}$ –star $(A_8)_4B_{30}$ mixtures where

the molecular weight of the solvophilic arm of $(A_{16})_4B_{30}$ copolymer is twice compared to the respective arm of the $(A_8)_4B_{30}$. The properties of interest are the critical micelle concentration, the mean aggregation number, the shape of the micelle which is expressed by the shape anisotropy, the thickness of the corona, and the solvophobic core radius. The simulation results revealed that the cmc values show a positive deviation from the ideal behavior. The interaction parameter $u \approx 0.5$ obtained from the activity coefficients could be attributed to the effective interactions between copolymers originated from the size asymmetry. This value lies between the previous findings for the effective interaction for the linear $A_{63}B_{30}$ –star $(A_{21})_3B_{30}$ ($u \approx 0.6$) and star $(A_{32})_2B_{30}$ –star $(A_{16})_4B_{30}$ ($u \approx 0.1$) mixtures arising only from architectural asymmetry between copolymers. The effective interactions slightly decrease the micelles's preferential aggregation number. The calculation of radial distribution functions $g(r)$ and the snapshot analysis reveal that the solvophilic parts of the copolymer chains are nonrandomly mixed in the corona. In addition, we studied star–H-shaped mixtures where the individual constituents form micelles with preferential and wide aggregation numbers and homo-linked-rings–linear mixtures where the individual constituents form wormlike and spherical micelles.

In the case of star $(A_{60})_2B_{30}$ –H-shaped $(A_{30})_2B_{30}(A_{30})_2$ mixtures our simulation results indicate that in mixtures with H-shaped molar fraction $[X_{\text{H-shaped}}] = 0.75$ the mass distribution remains monotonic and mixed micelles with wide aggregation numbers are formed. For mixtures having $[X_{\text{H-shaped}}] = 0.50$ the mass distribution forms almost a plateau and then decays slowly. Further decrease of H-shaped molar fraction, $[X_{\text{H-shaped}}] = 0.25$, leads to the formation of micelles with preferential aggregation number.

The pure homo-linked-rings solution forms wormlike micelles with high aggregation number while the smaller micelles are elongated spheres. Mixtures containing 10% and 20% linear diblock copolymers which have the same molecular weight as linked-rings copolymer form micelles similar to those of the pure linked rings. For mixtures having $[X_{\text{linear}}] = 0.50$, the preferential micelles are spherical while wormlike micelles are formed for slightly higher aggregation numbers.

-
- [1] S. Pispas, Y. Poulos, and N. Hadjichristidis, *Macromolecules* **31**, 4177 (1998).
- [2] P. M. Nguyen and P. T. Hammond, *Langmuir* **22**, 7825 (2006).
- [3] N. W. Suck and M. H. Lamm, *Langmuir* **24**, 3030 (2008).
- [4] C. Georgiadis, O. Moulτος, L. N. Gergidis, and C. Vlahos, *Langmuir* **27**, 835 (2011).
- [5] S. Pispas, N. Hadjichristidis, and J. W. Mays, *Macromolecules* **29**, 7378 (1996).
- [6] O. Moulτος, L. N. Gergidis, and C. Vlahos, *Macromolecules* **43**, 6903 (2010).
- [7] H. Iatrou, L. Willner, N. Hadjichristidis, A. Halperin, and D. Richter, *Macromolecules* **29**, 581 (1996).
- [8] Y. Sheng, C. Nung, and H. Tsao, *J. Phys. Chem. B* **110**, 21643 (2006).
- [9] G. Shi and C. Pan, *J. Polym. Sci., Part A: Polym. Chem.* **47**, 2620 (2009).
- [10] A. Kalogirou, O.A. Moulτος, L. N. Gergidis, and C. Vlahos, *Macromolecules* **47**, 5851 (2014).
- [11] G. Shi, L. Yang, and C. Pan, *J. Polym. Sci., Part A: Polym. Chem.* **46**, 6496 (2008).
- [12] X. Fan, B. Huang, G. Wang, and J. Huang, *Macromolecules* **45**, 3779 (2012).
- [13] T. Isono, Y. Satoh, K. Miyachi, Y. Chen, S. Sato, K. Tajima, T. Satoh, and T. Kakuchi, *Macromolecules* **47**, 2853 (2014).
- [14] E. B. Zhulina and O. V. Borisov, *ACS Macro Lett.* **2**, 292 (2013).
- [15] E. B. Zhulina and O. V. Borisov, *Macromolecules* **45**, 4429 (2012).
- [16] O. V. Borisov, E. B. Zhulina, F. Leermakers, M. Ballauff, and A. Muller, *Adv. Polym. Sci.* **241**, 1 (2011).

- [17] M. Hafezi and F. Sharif, *Langmuir* **28**, 16243 (2012).
- [18] A. B. Ebrahim Attia, Z. Y. Ong, J. L. Hedrick, P. P. Lee, P. L. R. Ee, P. T. Hammond, and Y. Yang, *Curr. Opin. Colloid Interface Sci.* **16**, 182 (2011).
- [19] R. Nagarajan, *Langmuir* **1**, 331 (1985).
- [20] N. Quarti, P. Viville, R. Lazzaroni, E. Minatti, M. Schappacher, A. Deffieux, J. L. Putaux, and R. Borsali, *Langmuir* **21**, 9085 (2005).
- [21] O. Moutos, L. N. Gergidis, A. Kalogirou, and C. Vlahos, *J. Polym. Sci., Part B: Polym. Phys.* **53**, 442 (2015).
- [22] C. C. Greenberg, M. D. Foster, C. M. Turner, S. Corona-Galvan, E. Cloutet, P. D. Butler, B. Hammouda, and R. P. Quirk, *Polymer* **40**, 4713 (1999).
- [23] C. C. Greenberg, M. D. Foster, C. M. Turner, S. Corona-Galvan, E. Cloutet, R. P. Quirk, P. D. Butler, and C. Hawker, *J. Polym. Sci., Part B: Polym. Phys.* **39**, 2549 (2001).
- [24] T. D. Martter, M. D. Foster, T. Yoo, S. Xu, G. Lizzaraga, R. P. Quirk, and P. D. Butler, *Macromolecules* **35**, 9763 (2002).
- [25] T. D. Martter, M. D. Foster, K. Ohno, and D. M. Haddleton, *J. Polym. Sci., Part B: Polym. Phys.* **40**, 1704 (2002).
- [26] T. D. Martter, M. D. Foster, T. Yoo, S. Xu, G. Lizzaraga, and R. P. Quirk, *J. Polym. Sci., Part B: Polym. Phys.* **41**, 247 (2002).
- [27] C. Vlahos and M. Kosmas, *Polymer* **44**, 503 (2003).
- [28] M. K. Kosmas and C. H. Vlahos, *J. Chem. Phys.* **119**, 4043 (2003).
- [29] C. Vlahos and M. Kosmas, *Macromolecules* **37**, 9184 (2004).
- [30] P. E. Theodorakis, A. Avgeropoulos, J. J. Freire, M. Kosmas, and C. Vlahos, *Macromolecules* **39**, 4235 (2006).
- [31] P. Polanowski and J. K. Jeszka, *Langmuir* **23**, 8678 (2007).
- [32] M. Murat and G. S. Grest, *Macromolecules* **29**, 1278 (1996).
- [33] S. Plimpton, *J. Comput. Phys.* **117**, 1 (1995).
- [34] S. Puvvada and D. Blankschtein, *J. Phys. Chem.* **96**, 5579 (1992).
- [35] G. K. Bourov and A. Bhattacharya, *J. Chem. Phys.* **123**, 204712 (2005).
- [36] M. Zaldivar and R. G. Larson, *Langmuir* **19**, 10434 (2003).
- [37] J. C. Sunshine and J. J. Green, *Nanomedicine* **8**, 1173 (2013).